√ Copy

TK7874 .R372 2002
chstx

OCLC ILL Number: 10389688

Jun 28, 2005 9:23 AM

Ariel: 130.85.150.114

Ship to:
University of Maryland, Baltimore Co
Kuhn Library & Gallery - ILL
1000 Hilltop Circle
Baltimore, MD 21250

Symbol: MUB

Email:
Phone:
Fax: 410 455-1061

Patron: DEPT; STATUS; Gobbert, Matthias

Lending String: *WAU,SFB,IXA,IXA,MYG

☐ Default / IFM / CC / MA / DA

Maxcost: $20IFM

Ariel
Direct Scanned ☐

Journal Title:
Rapid thermal and other short-time processing technologies III ; proceedings of the International Symposium / (Pennington, NJ ; Electrochemical Society)

Volume: 2002-11 **Issue:** **Month/Year:** 2002 **Pages:** 81-88 copy of chapter

Article:
International Symposium on Rapid Thermal and Other Short-Time Processing Technologies (3rd ; 2002 ; Samuel G. Webster, Matthias K. Gobbert, and Timothy S. Cale; Transient 3-D/3-D Transport and Reactant-Wafer Interactions; Adsorption and Desorption

Copyright: CCG

Notes: Borrowing Notes; Please scan color items in color when possible. MD Network Request. Do Not Charge. Patron wants copy of chapter. Thanks

OCLC #: 51849725

UWE #: L147383

UWorld Express
Univ of Washington Libraries
Box 352900
Seattle, WA 98195-2900

(206) 543-1878 / (800) 324-5351
uworld@u.washington.edu
www.uworldexpress.info
Fax: (206) 685-8049

Your OCLC IFM account has been charged $15.00

Rapid Thermal and Other Short-Time Processing Technologies III

Proceedings of the International Symposium

Editors

P. J. Timans
Mattson Technology
Fremont, California, USA

E. Gusev
IBM Thomas Watson Research Center
Yorktown Height, New York, USA

F. Roozeboom
Philips Research
Eindhoven, The Netherlands

M. C. Öztürk
North Carolina State University
Raleigh, North Carolina, USA

D.-L. Kwong
University of Texas
Austin, Texas, USA

Sponsoring Divisions:
Electronics, Dielectric Science and Technology, and High Temperature Materials

Proceedings Volume 2002-11

THE ELECTROCHEMICAL SOCIETY, INC.
65 South Main St., Pennington, NJ 08534-2839, USA

Copyright 2002 by The Electrochemical Society, Inc.
All rights reserved.

This book has been registered with Copyright Clearance Center, Inc.
For further information, please contact the Copyright Clearance Center,
Salem, Massachusetts.

Published by:

The Electrochemical Society, Inc.
65 South Main Street
Pennington, New Jersey 08534-2839, USA

Telephone 609.737.1902
Fax 609.737.2743
e-mail: ecs@electrochem.org
Web: www.electrochem.org

Library of Congress Catalogue Number: 2002111727

ISBN 1-56677-334-2

Printed in the United States of America

The internatio
Technologies
Pennsylvania a
For the fourth
thermal proces
with 54 papers
annual symposi
working in the
RTP, Atomic L
focus of the pro
and applications

This book cont
contents the rea
lowering the th
dielectrics in na
budget heating t
flows and flash R

A panel discussi
materials process
Technology Road
whether the techn
scale in just a few
– as usual – a l
Instruments), M. C
S. Guha (IBM), an

Finally, the editors
ECS Divisions (El
Materials Division
International, Axc
Lighting (France),
'traditional' core o
high level of our sy

TRANSIENT 3-D/3-D TRANSPORT AND REACTANT-WAFER INTERACTIONS: ADSORPTION AND DESORPTION

Samuel G. Webster*[1], Matthias K. Gobbert*[2], and Timothy S. Cale†[2]

*Department of Mathematics and Statistics
University of Maryland, Baltimore County
1000 Hilltop Circle
Baltimore, MD 21250

†Focus Center — New York, Rensselaer:
Interconnections for Gigascale Integration
Rensselaer Polytechnic Institute, CII 6015
110 8th Street
Troy, NY 12180-3590

NOTICE: This material may be protected by copyright law (Title 17 U S Code)

Atomic layer deposition (ALD) has shown the ability to deposit uniform film layers in high aspect ratio features. This ability makes ALD a vital component of integrated circuit fabrication. We present a three-dimensional extension of a previously developed deterministic transport and reaction model for ALD. At the wafer surface, the transport model is given by the Boltzmann transport equation for gas dynamics and the surface reaction model is based on reversible Langmuir expressions. In this paper, we present 3-D simulations for a single-species model during a reversible adsorption step on the feature scale. Number density results are seen to be consistent with those found in previously conducted 2-D studies. Uniform flux and surface coverage are also demonstrated.

INTRODUCTION

Atomic Layer Deposition (ALD) has been shown to provide excellent film thickness uniformity over severe topography, namely in high aspect ratio features found in modern integrated circuit (IC) fabrication. In an ideal ALD process, the deposition of solid material on the feature surface is accomplished one atomic or monolayer at a time, in a self-limiting fashion which allows for complete control of film thickness. A representative process consists of a controlled sequence of reactant flows and reactor purges. Initially, a gaseous species (A) is fed into the reactor and (ideally) one molecular layer adsorbs onto the wafer surface. After purging the reactor, a second gaseous species (B) is fed into the reactor and reacts with the adsorbed layer of (A) to form the next layer of film. This sequence is repeated until a film

[1]Electrochemical Society Student Member
[2]Electrochemical Society Active Member

of uniform thickness has been deposited [1, 2]. This ALD process is described by a fully transient, Boltzmann equation based transport and reaction model. We outline the model in the next section and briefly describe the numerical approach in the following section. We then present 3-D simulation results for a reversible adsorption step in the ALD process.

THE MODEL

The spatial domain Ω of the model consists of the gas-filled region inside an individual feature of typical size less than 1 μm and a small volume above the feature mouth. Typical operating conditions are assumed to be $P = 1$ torr and $T = 500$ K. The flow of the gaseous species $i = 0, 1, \ldots, n_s$ is then described by a system of Boltzmann equations [3, 4, 5, 6], stated here already in dimensionless form as

$$\frac{\partial f^{(i)}}{\partial t} + v \cdot \nabla_x f^{(i)} = \frac{1}{\text{Kn}} \sum_{j=0}^{n_s} Q_{ij}(f^{(i)}, f^{(j)}), \quad i = 0, 1, \ldots, n_s, \tag{1}$$

where the collision operators $Q_{ij}(f^{(i)}, f^{(j)})$ model the collisions between molecules of gaseous species i and j. The left-hand side of Eq. 1 describes the convective transport of the gaseous species. The right-hand side of the Boltzmann equation models the effect of collisions among molecules. The unknown variables are the density distribution functions $f^{(i)}(x, v, t)$, that give the scaled probability density that a molecule i is at position $x = (x_1, x_2, x_3) \in \Omega \subset \mathbb{R}^3$ with velocity $v = (v_1, v_2, v_3) \in \mathbb{R}^3$ at time $t \geq 0$; they have to be determined for all points of $x \in \Omega$, for all possible velocities $v \in \mathbb{R}^3$, and for all times $t \geq 0$. The velocity integral of $f^{(i)}(x, v, t)$ gives the dimensionless number density of the reactive species $c_i(x, t) = \int f^{(i)}(x, v, t)\, dv$, for $i = 0, 1, \ldots, n_s$.

Using the assumption that the reactive species $j = 1, \ldots, n_s$ are at least one order of magnitude less dense than the inert carrier gas $j = 0$, it is possible to decouple the equation for $i = 0$ from the remaining ones for reactive species [5, 6]. This assumption is justified for many common processes used in IC fabrication. This reduces the problem to solving the system in Eq. 1 for the reactive species $i = 1, \ldots, n_s$.

For domains on the scale of features, we additionally use the fact that the Knudsen number Kn is large compared to unity and, hence, the transport is free molecular flow given by Eq. 1 with a zero right-hand side. Specifically, the Knudsen number is defined as the ratio of the mean free path λ over the typical length scale L^* of the domain. With an operating pressure of $P = 1$ torr and temperature of $T = 500$ K, we obtain a mean free path of $\lambda \simeq 100$ μm. With $L^* = 1$ μm for feature scale models, a Knudsen number of Kn $\simeq 100$ is obtained; consequently the Boltzmann equation for free molecular transport.

The domain Ω of the studies in this paper consists of the interior of a trench corner and a layer of the gas domain above the feature mouth; a schematic of the

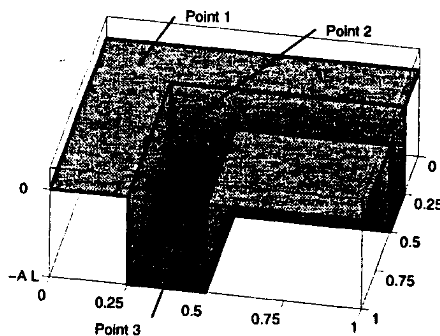

Figure 1: Schematic of domain with width $L = 0.25\ \mu$m and aspect ratio A defining the points of interest. All lengths shown are in microns.

domain is presented in Figure 1. We model the inflow at the top of the domain above the feature mouth by prescribing a Maxwellian velocity distribution. We assume specular reflection at the vertical ends of the feature to simulate a corner of two semi-infinite trenches. Along the remainder of the boundary, which represents the wafer surface of the feature, the following reaction model is used to describe the adsorption of molecules to the surface. The adsorption and desorption of species A and the reaction of species B with adsorbed molecules of A is modeled by

$$\mathrm{A} + (\mathrm{v}) \rightleftharpoons \mathrm{A_v}, \tag{2}$$

$$\mathrm{A_v} + \mathrm{B} \longrightarrow (\mathrm{v}) + (*), \tag{3}$$

where $\mathrm{A_v}$ is the adsorbed species A, (v) is an available surface site and $(*)$ denotes the non-adsorbing gaseous product; The product of gaseous B with adsorbed A forms an available surface site (v).

The dimensionless reaction rates then become

$$R_1 = \gamma_1^f\,(1 - \vartheta_A)\,\eta_1(x,t) - \gamma_1^b\,\vartheta_A \tag{4}$$

$$R_2 = \gamma_2^f\,\vartheta_A\,\eta_2(x,t) \tag{5}$$

with γ_1^f and γ_1^b denoting the reaction rate coefficients for adsorption and desorption of A in Reaction 1, respectively, and γ_2^f denoting the rate coefficient for reaction of B with $\mathrm{A_v}$ during Reaction 2. The fraction of the wafer surface that is occupied by adsorbed molecules of species A is the surface coverage, $0 \le \vartheta_A \le 1$.

The flux of species A and B to the surface are denoted by η_1 and η_2, respectively. If we assume that molecules re-emitted from the wafer surface possess a Maxwellian velocity distribution, the boundary condition at the wafer surface becomes

$$f^{(1)}(x,v,t) = [\eta_1(x,t) - R_1(x,t)]\,C_1(x)\,M_1^{ref}(v), \quad \nu \cdot v < 0, \tag{6}$$

$$f^{(2)}(x,v,t) = [\eta_2(x,t) - R_2(x,t)]\,C_2(x)\,M_2^{ref}(v), \quad \nu \cdot v < 0. \tag{7}$$

The factors C_i are chosen such that in the absence of reactions ($R_k = 0$), mass is conserved; i.e., influx equals outflux for each species.

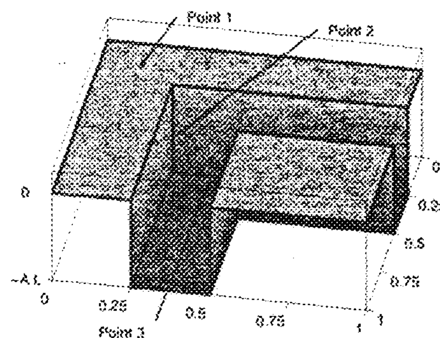

Figure 1: Schematic of domain with width $L = 0.25$ μm and aspect ratio A defining the points of interest. All lengths shown are in microns.

domain is presented in Figure 1. We model the inflow at the top of the domain above the feature mouth by prescribing a Maxwellian velocity distribution. We assume specular reflection at the vertical ends of the feature to simulate a corner of two semi-infinite trenches. Along the remainder of the boundary, which represents the wafer surface of the feature, the following reaction model is used to describe the adsorption of molecules to the surface. The adsorption and desorption of species A and the reaction of species B with adsorbed molecules of A is modeled by

$$\mathrm{A} + (\mathrm{v}) \rightleftharpoons \mathrm{A_v}, \tag{2}$$

$$\mathrm{A_v} + \mathrm{B} \rightarrow (\mathrm{v}) + (*), \tag{3}$$

where $\mathrm{A_v}$ is the adsorbed species A, (v) is an available surface site and $(*)$ denotes the non-adsorbing gaseous product; The product of gaseous B with adsorbed A forms an available surface site (v).

The dimensionless reaction rates then become

$$R_1 = \gamma_1^f (1 - \vartheta_A)\, \eta_1(x,t) - \gamma_1^b \vartheta_A \tag{4}$$

$$R_2 = \gamma_2^f \vartheta_A\, \eta_2(x,t) \tag{5}$$

with γ_1^f and γ_1^b denoting the reaction rate coefficients for adsorption and desorption of A in Reaction 1, respectively, and γ_2^f denoting the rate coefficient for reaction of B with $\mathrm{A_v}$ during Reaction 2. The fraction of the wafer surface that is occupied by adsorbed molecules of species A is the surface coverage, $0 \leq \vartheta_A \leq 1$.

The flux of species A and B to the surface are denoted by η_1 and η_2, respectively. If we assume that molecules re-emitted from the wafer surface possess a Maxwellian velocity distribution, the boundary condition at the wafer surface becomes

$$f^{(1)}(x,v,t) = [\eta_1(x,t) - R_1(x,t)]\, C_1(x)\, M_1^{ref}(v), \quad \nu \cdot v < 0, \tag{6}$$

$$f^{(2)}(x,v,t) = [\eta_2(x,t) - R_2(x,t)]\, C_2(x)\, M_2^{ref}(v), \quad \nu \cdot v < 0. \tag{7}$$

The factors C_i are chosen such that in the absence of reactions ($R_k = 0$), mass is conserved; i.e., influx equals outflux for each species.

THE NUMERICAL METHOD

To numerically solve Eq. 1 with the given boundary conditions and initial condition, the unknowns $f^{(i)}$ for the reactive species are expanded in velocity space with respect to judiciously chosen basis functions [5, 7, 8]. The resulting system of linear hyperbolic transport equations is then solved using the discontinuous Galerkin method (DGM) [9] using the code DG [10] as a hyperbolic solver.

RESULTS

In this section, we report results for the reversible adsorption step of a representative ALD cycle. All simulations use the single-species version ($n_s = 1$) of the reaction model, since only A is fed into the reactor during adsorption. The dimensionless adsorption rate coefficients are fixed: $\gamma_1^f = 10^{-2}$ and $\gamma_1^b = \gamma_1^f/100$. These values correspond to relatively few molecules adsorbing to the wafer surface; hence most are re-emitted from the boundary. We have obtained results for several different aspect ratios ($A = 1, 2, 3$) for the geometries of the type shown in Figure 1; for presentation purposes only results for $A = 2, 3$ will be shown. The width of the feature mouth is fixed at $L = 0.25\,\mu$m. Initially, the feature is assumed to be free of reactive gas. The reactive gas is then fed into the feature from above and, eventually, the feature fills with gas. Our choice of γ_1^f dictates that only a small amount of the gas will adsorb on the wafer surface.

Figure 2 shows slice plots of the dimensionless number density of species A throughout a corner trench with an aspect ratio $A = 2$ at several (re-dimensionalized) points in time. Each slice is a horizontal cross-section through the trench at a fixed height x_3, thus the shape of the slices outline the shape of the domain. The top-most slice is chosen at $x_3 = 0$ just above the feature mouth, hence it does not have the outline of the corner trench like the remaining slices. The color of the finite elements on the slice represents a gray scale image of the dimensionless number density c throughout that cross-section through the domain, ranging from light color for $c = 0$ to dark color for $c = 1$. Figure 2 (a) plots this number density at time $t = 2$ ns; this shows that transport from the interface to the flat wafer surface is very fast. Initially, the number density is higher at the flat wafer surface since the molecules have not yet traveled down through the domain. Observe the lighter shading of the L-shaped area above the feature mouth as compared to the rest of the area above the feature mouth. A lower number density is seen here since the gas is gravitating toward the bottom of the wafer surface. Figures 2 (b) and (c) show number density at times $t = 4$ ns and $t = 8$ ns, respectively. Notice the lighter shadings of the slice planes near the bottom of the feature as compared to the layer above the wafer surface. This represents the fact that it takes longer times for the gas to reach the bottom of the feature. As Figure 2 (d) demonstrates, it takes slightly longer than 16 ns for a feature with aspect ratio $A = 2$ to fill with gas.

To determine the flux and fractional surface coverage over time, several points on the wafer surface of the trench were chosen in the domain shown in Figure 1.

Point 1 is located on the flat area of the wafer surface above the mouth of the feature $(x_1, x_2, x_3) = (.125, .125, 0)$. Point 2 lies along the corner of the wafer surface half-way down the trench with $(.25, .25, -0.5AL)$. Point 3 is located along the bottom of the feature at $(.375, .375, -AL)$. It is expected that coverage will increase fastest at Point 1 since it lies closest to the gas-phase interface. Similarly, the coverage will increase the slowest at Point 3 since it takes longer times for the gas to reach the wafer surface at the bottom of the feature. Figures 3 (a) and (b) show the flux η vs. time and surface coverage ϑ_A vs. time for $\gamma_1^f = 10^{-2}$. The final time is $t_{fin} = 250$ ns. Figure 3 (a) shows that the fluxes at Points 1, 2, 3 tend to approximately the same equilibrium value. The lag in the time to reach the respective steady-state value is again explained by the extra time necessary for the gas to reach the points located within the trench. Figure 3 (b) shows the fractional surface coverage at the three selected points. Observe that although the feature has filled with gas at $t = 16$ ns (see Figure 2 (d)), full coverage has not nearly been achieved yet. This is explained by the selection of $\gamma_1^f = 10^{-2}$. A negligible fraction of the molecules adsorb onto the wafer surface as compared to the fraction that re-emit into the feature. Observe that the evolution of ϑ_A is still in its linear regime.

Figure 4 shows slice plots of dimensionless number density of species A throughout a corner trench with aspect ratio $A = 3$. Immediately, we can expect longer times for complete feature fill due to the larger volume of the feature. Figure 4 (a) shows the dimensionless number density at $t = 5$ ns. The lag in time necessary for complete feature fill is already apparent even after only $t = 5$ ns. Figures 4 (b) and (c) shows the number density of species A at $t = 10$ ns and $t = 20$ ns, respectively. Figure 4 (d) shows that for an aspect ratio of $A = 3$, it takes approximately $t = 80$ ns for the trench to entirely fill with gas.

Figures 5 (a) and (b) show the flux and surface coverage for a corner trench with aspect ratio $A = 3$. As expected, greater lags are seen due to the larger volume of the domain. Figure 5 (a) shows the near-uniform flux to the wafer surface at Points 1, 2, and 3. Steady-state is still rapidly achieved although not as quickly as seen in Figure 3 (a). Figure 5 (b) shows the fractional surface coverage at each of the three selected points. Observe that the evolution of the fractional surface coverage is still in its linear regime. As with the flux there is an even greater lag seen for this higher aspect ratio.

CONCLUSIONS

A fully three-dimensional model and numerical method have been presented that simulate the transient behavior of a reversible adsorption step of a representative ALD process. Results were shown that predict number density, flux to the surface, and fractional surface coverage at several points along a trench corner for a single species model with realistic adsorption rate. The results obtained in this paper are seen to be consistent with those found in previously conducted 2-D studies [4, 5] and will enable the extension of previous predictive studies using the multi-species model for full ALD cycles from 2-D to 3-D [6, 11, 12].

ACKNOWLEDGMENTS

The authors acknowledge the support from the University of Maryland, Baltimore County for the computational hardware used for this study. Prof. Cale acknowledges support from MARCO, DARPA, and NYSTAR through the Interconnect Focus Center.

REFERENCES

[1] M. Ritala, M. Leskela, *Nanotechnology* **10**, 19 (1999).

[2] T. Suntola, *Thin Solid Films* **216**, 84 (1992).

[3] C. Cercignani, *The Boltzmann Equation and Its Applications*, vol. 67, *Applied Mathematical Sciences*, (Springer-Verlag, 1988).

[4] M. K. Gobbert, T. S. Cale. A feature scale transport and reaction model for atomic layer deposition. In *Fundamental Gas-Phase and Surface Chemistry of Vapor-Phase Deposition II* (2001), M. T. Swihart, M. D. Allendorf, and M. Meyyappan, Eds., vol. 2001-13, The Electrochemical Society Proceedings Series, pp. 316–323.

[5] M. K. Gobbert, S. G. Webster, T. S. Cale. Transient adsorption and desorption in micron scale features. *J. Electrochem. Soc.*, in press.

[6] M. K. Gobbert, V. Prasad, T. S. Cale. Modeling and simulation of atomic layer deposition at the feature scale. *J. Vac. Sci. Technol. B*, in press.

[7] M. K. Gobbert, S. G. Webster, J.-F. Remacle, T. S. Cale. A spectral Galerkin ansatz for the deterministic solution of the Boltzmann equation on irregular domains. In preparation.

[8] C. Ringhofer, *Acta Numerica* **6**, 485 (1997).

[9] B. Cockburn, G. E. Karniadakis, C.-W. Shu, Eds., *Discontinuous Galerkin Methods: Theory, Computation and Applications*, vol. 11, *Lecture Notes in Computational Science and Engineering*, (Springer-Verlag, 2000).

[10] J.-F. Remacle, J. Flaherty, M. Shephard. An adaptive discontinuous Galerkin technique with an orthogonal basis applied to Rayleigh-Taylor flow instabilities. *SIAM J. Sci. Comput.*, accepted.

[11] M. K. Gobbert, V. Prasad, T. S. Cale. A feature scale model for atomic layer deposition. In *Proceedings of the* Eighteenth International VLSI Multilevel Interconnection Conference, *VMIC 01 IMIC-300* (2001), pp. 413–417.

[12] M. K. Gobbert, V. Prasad, T. S. Cale. Predictive modeling of atomic layer deposition on the feature scale. *Thin Solid Films*, in press.

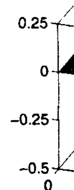

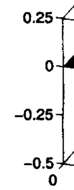

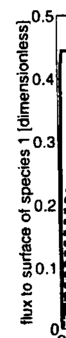

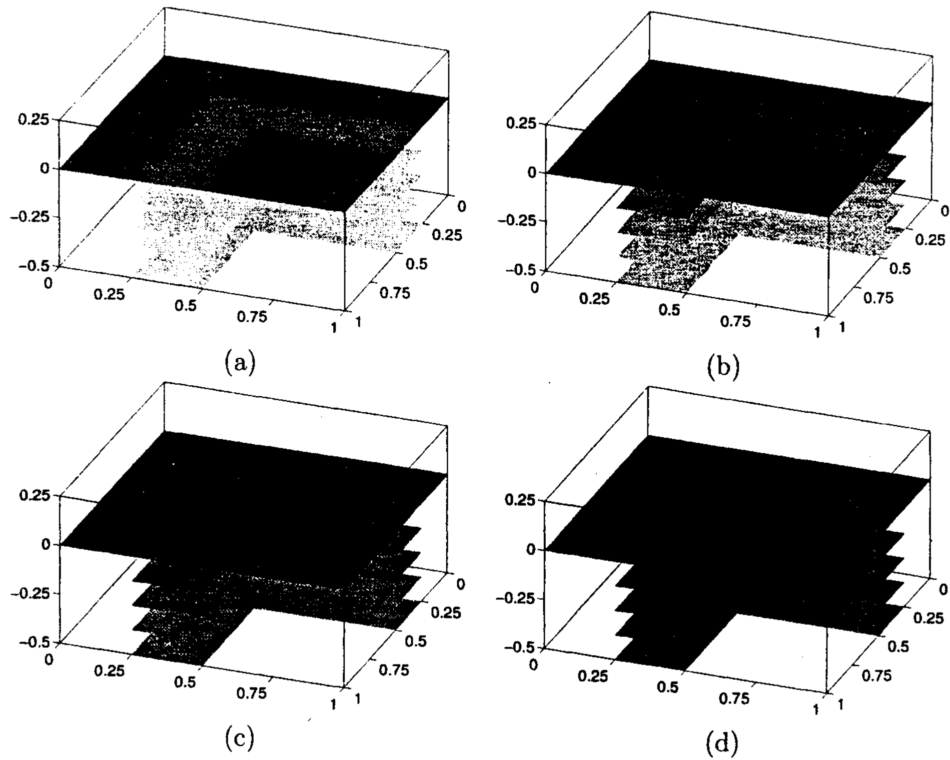

Figure 2: Dimensionless number density in a trench corner with aspect ratio $A = 2$ at times (a) 2 ns, (b) 4 ns, (c) 8 ns, (d) 16 ns. Different shades indicate dimensionless number density. Note the symmetry among the x_1, x_2 axes. The vertical axis corresponds to x_3. All lengths shown are in microns.

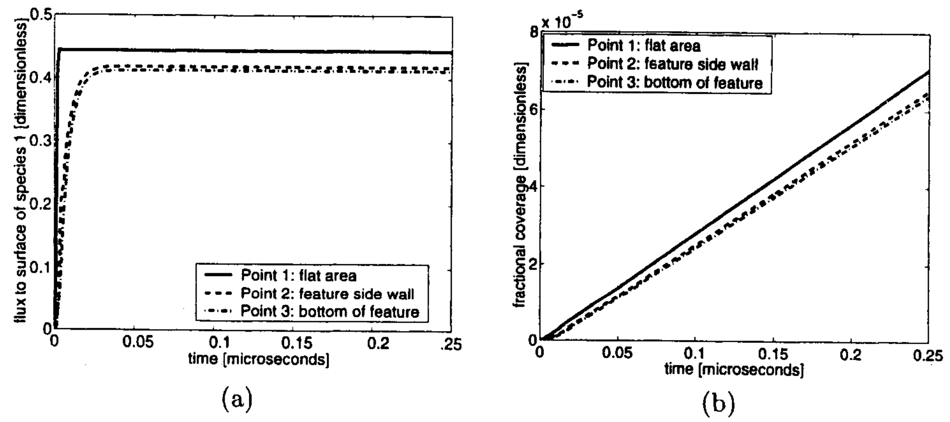

Figure 3: (a) Dimensionless flux to the surface of species A and (b) fractional surface coverage for $\gamma_1^f = 10^{-2}$ in a trench corner with aspect ratio $A = 2$.

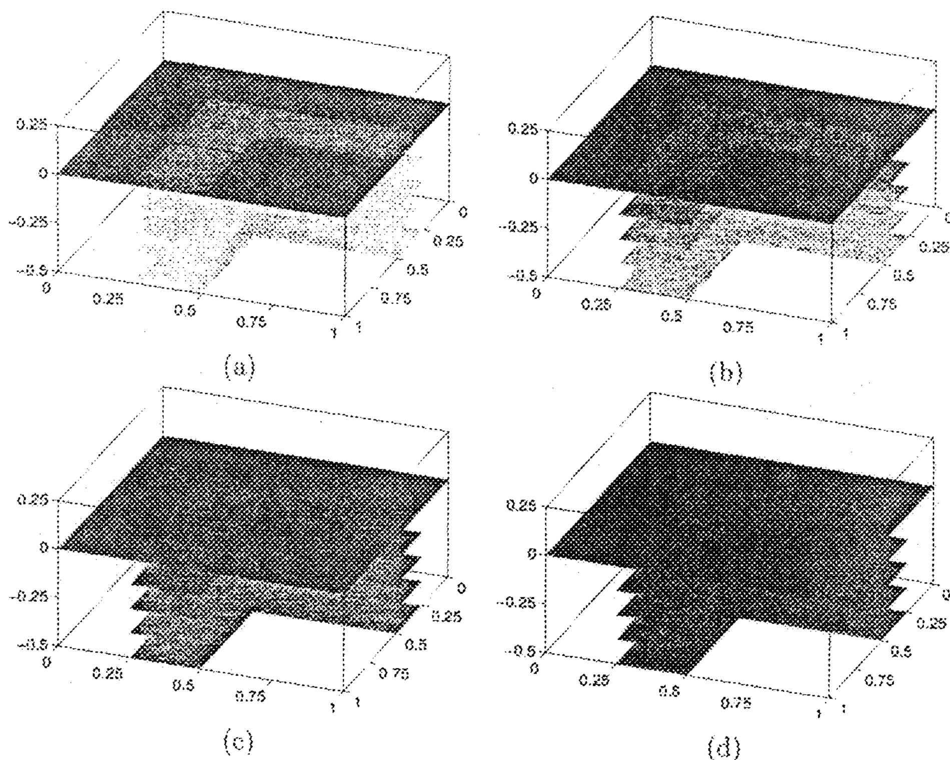

Figure 2: Dimensionless number density in a trench corner with aspect ratio $A = 2$ at times (a) 2 ns, (b) 4 ns, (c) 8 ns, (d) 16 ns. Different shades indicate dimensionless number density. Note the symmetry among the x_1, x_2 axes. The vertical axis corresponds to x_3. All lengths shown are in microns.

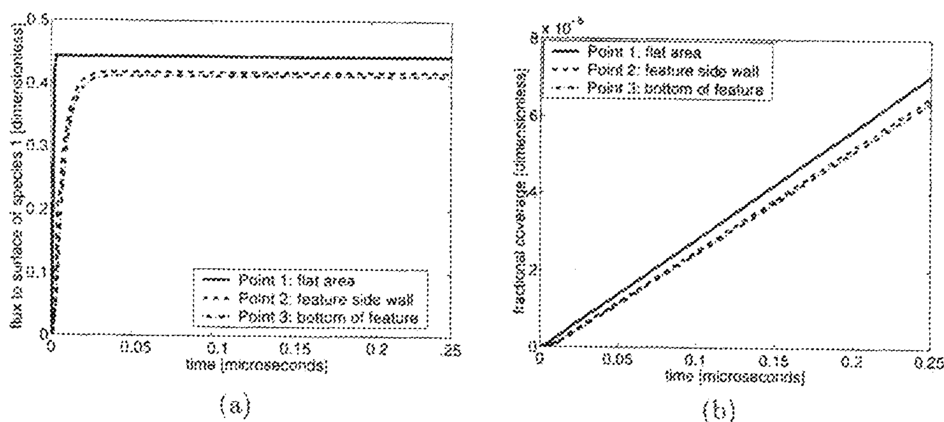

Figure 3: (a) Dimensionless flux to the surface of species A and (b) fractional surface coverage for $\gamma_1^f = 10^{-2}$ in a trench corner with aspect ratio $A = 2$.

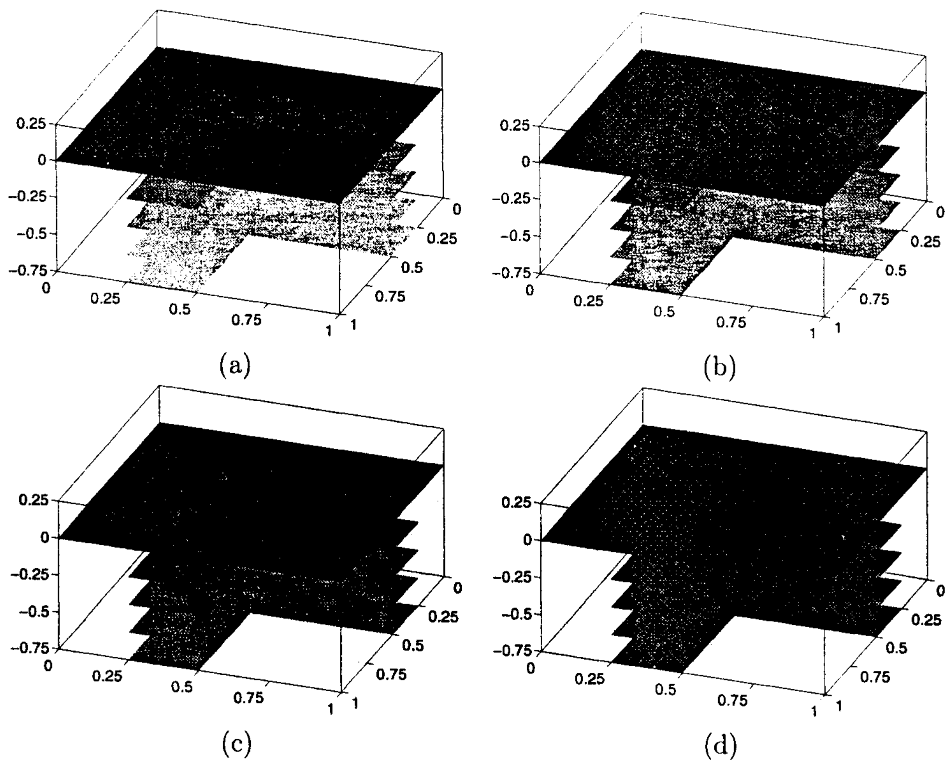

Figure 4: Dimensionless number density in a trench corner with aspect ratio $A = 3$ at times (a) 5 ns, (b) 10 ns, (c) 20 ns, (d) 80 ns. Different shades indicate dimensionless number density. Note the symmetry among the x_1, x_2 axes. The vertical axis corresponds to x_3. All lengths shown are in microns.

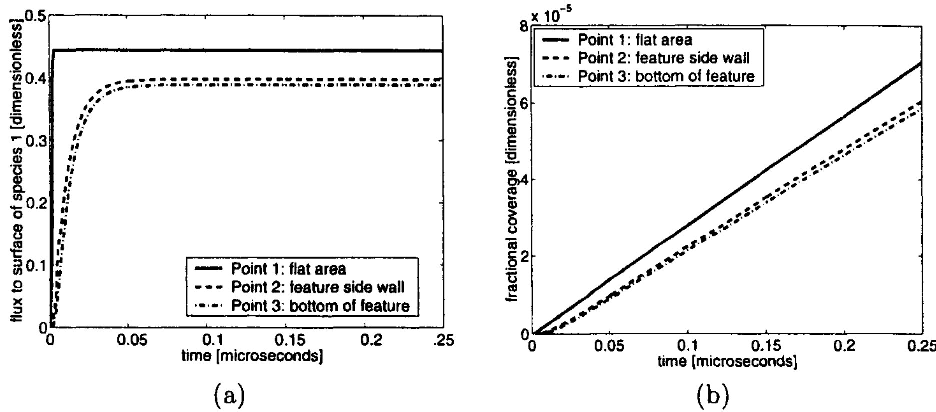

Figure 5: (a) Dimensionless flux to the surface of species A and (b) fractional surface coverage for $\gamma_1^f = 10^{-2}$ in a trench corner with aspect ratio $A = 3$.

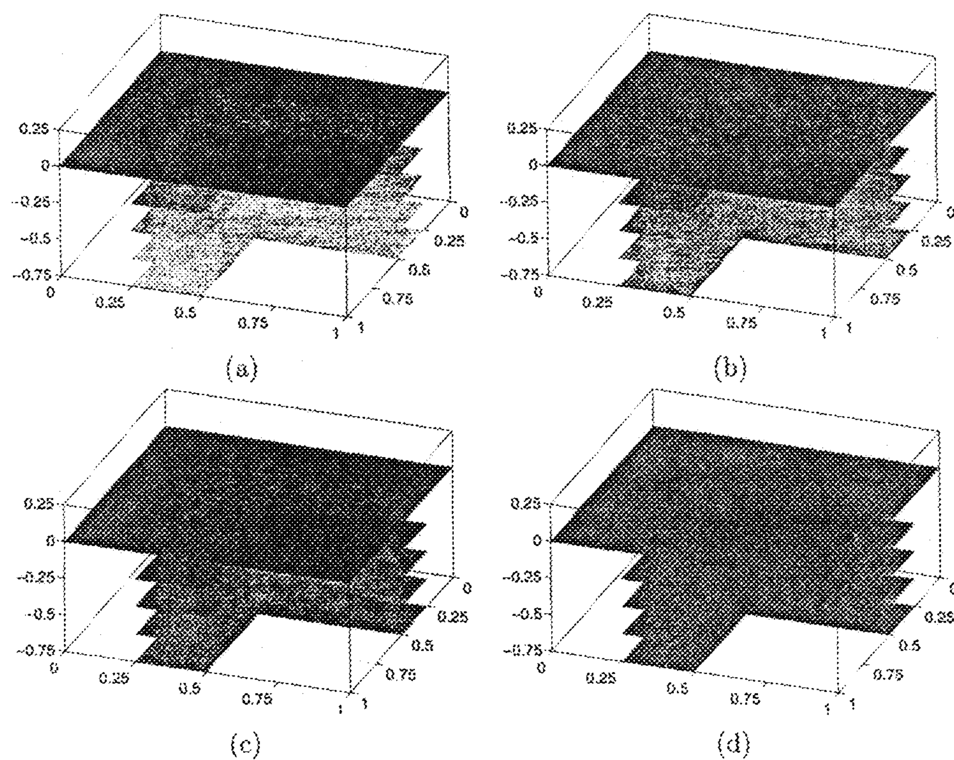

Figure 4: Dimensionless number density in a trench corner with aspect ratio $A = 3$ at times (a) 5 ns, (b) 10 ns, (c) 20 ns, (d) 80 ns. Different shades indicate dimensionless number density. Note the symmetry among the x_1, x_2 axes. The vertical axis corresponds to x_3. All lengths shown are in microns.

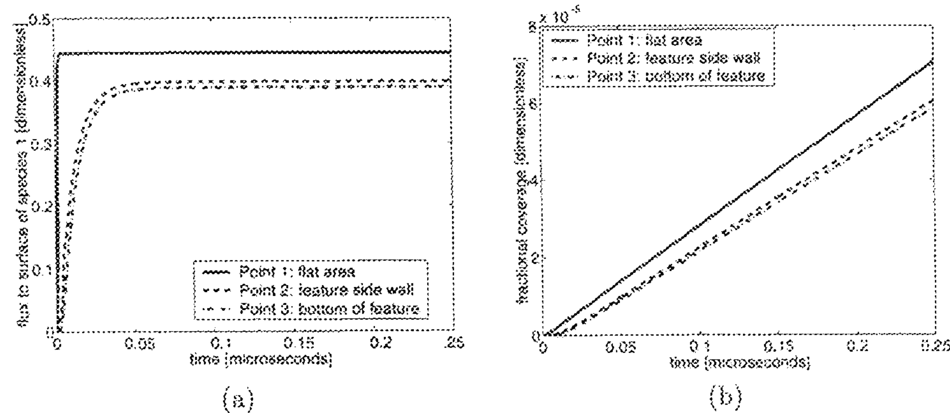

Figure 5: (a) Dimensionless flux to the surface of species A and (b) fractional surface coverage for $\gamma_1^f = 10^{-2}$ in a trench corner with aspect ratio $A = 3$.